https://doi.org/10.5194/essd-2026-779
Preprint. Discussion started: 23 November 2026
© Author(s) 2026. CC BY 4.0 License.



Open Access Earth System Science Data Discussions

A multi-year stable isotope dataset of precipitation and groundwater and new hydroisotopic indices for assessing isotopic signal integration in the Sierra de Segura karst aquifer system, southern Spain

Antonio Lope Morales González [1], Jorge Jódar[1], Antonio González Ramón[1], Francisco Moral Martos[2], Rosario Jiménez Espinosa [3] y Fernando Gázquez[4].

[1] Instituto Geológico y Minero de España (IGME-CSIC): al.morales@igme.es j.jodar@igme.es, antonio.gonzalez@igme.es
[2] Universidad Pablo de Olavide: fmormar@upo.es
[3] Departamento de Geología de la Universidad de Jaén; respino@ujaen.es
[4] Universidad de Almería: f.gazquez@ual.es
Correspondence to: *Antonio Lope Morales González* (al.morales@igme.es)

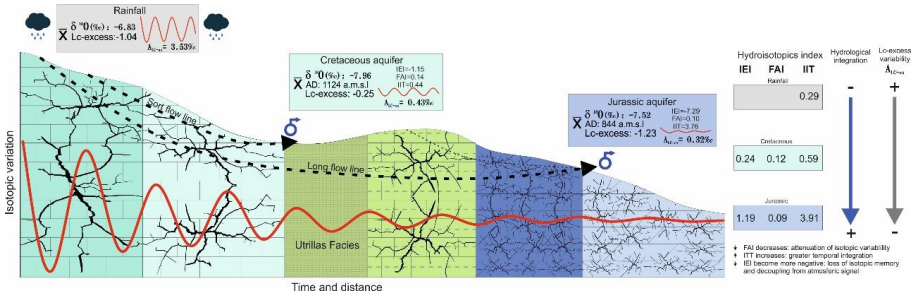

Abstract

Stable isotope observations of precipitation and groundwater provide valuable information for characterizing recharge processes, groundwater mixing, and the temporal integration of hydrological signals, but long-term paired datasets remain relatively scarce in Mediterranean karst systems. Here, we present a multi-year precipitation–groundwater stable isotope dataset from the Sierra de Segura multilayer karst aquifer system in southern Spain. The dataset comprises 884 water samples collected between 2017 and 2023, including 403 precipitation samples from eight collectors distributed along an elevation gradient between 550 and 1800 m a.s.l., and 481 groundwater samples from 20 springs draining the Upper Cretaceous (n = 11) and Jurassic (n = 9) aquifers. Stable isotope compositions of $\delta^{18}O$ and $\delta^{2}H$ were determined by cavity ring-down spectroscopy and normalized to the VSMOW scale. The dataset includes sampling metadata and derived isotopic variables, including d-excess and local line-conditioned excess (Lc-ex), allowing the temporal and spatial variability of the isotopic signal to be assessed across the precipitation–groundwater continuum. In addition, three hydroisotopic indices are introduced as comparative descriptors of isotopic signal transformation within the aquifer system: the Isotopic Environmental Integration Index (IEI), the Isotopic Attenuation Factor (IAF), and the Temporal Integration Index (TII). These indices quantify complementary aspects of the modification, attenuation, and temporal integration of the precipitation-derived isotopic signal and are not intended as direct estimates of groundwater age or mean transit time. The dataset and derived indices provide a structured basis for investigating isotope attenuation, recharge dynamics, groundwater mixing, and hydrological integration in Mediterranean karst aquifers, and facilitate comparison with isotope datasets from other hydrogeological settings. The complete dataset and associated metadata are made available through a persistent open-access repository to support data reuse and reproducible research.

Keywords: Local deuterium excess, hierarchical recharge, hydrological integration, hydroisotopic index, carbonate aquifers.

https://doi.org/10.5194/essd-2026-779
Preprint. Discussion started: 23 November 2026
© Author(s) 2026. CC BY 4.0 License.



1. Introduction

In semi-arid regions, the long-term sustainability of groundwater resources largely depends on the ability of aquifer systems to store and integrate recharge, which is highly variable in both space and time (Custodio, E. 2019). Marked seasonality in precipitation, high potential evapotranspiration, and increasing climatic variability pose major challenges for quantifying groundwater recharge mechanisms and transit processes in contemporary hydrogeology (Jódar et al., 2020; Bouchaou et al., 2024; Sorensen et al., 2024; Turkeltaub and Bel, 2024; Ghosh et al., 2025; Siyad et al., 2025; Morales González et al., 2026). This challenge is particularly relevant in stratified aquifer systems, where the coexistence of multiple permeable units may promote indirect recharge, inter-aquifer mixing, and contrasting groundwater transit behaviors.

Stable water isotopes ($\delta^{18}O$ and $\delta^{2}H$) are widely used to investigate groundwater recharge, flow paths, and mixing processes (Dansgaard, 1964; Gat, 1996; Clark and Fritz, 1997; Yanes and Moral, 2022; Morales González et al., 2024). Traditionally, deuterium excess (d-excess) provides information on evaporation conditions in moisture source regions (Rozanski et al., 1993; Pfahl and Sodemann, 2014). However, in semi-arid Mediterranean environments, the isotopic composition of precipitation may be substantially modified by post-condensation processes, including below-cloud evaporation, partial raindrop re-evaporation, and soil-water evaporation prior to infiltration, thereby obscuring the original atmospheric isotopic signal.

In this context, the local line-conditioned deuterium excess (Lc-ex), defined as the deviation of a water sample from the Local Meteoric Water Line (LMWL), has emerged as a sensitive indicator of post-condensation isotopic modification (Araguás-Araguás et al., 2000; Froehlich et al., 2002; Cardona-Hernández et al., 2026). While its usefulness in identifying evaporative processes in precipitation has been widely demonstrated, its application to groundwater systems is limited.

Because Lc-ex is expected to be progressively attenuated by infiltration, mixing, and groundwater storage, it may provide a useful tracer of recharge integration and isotopic signal transformation within multilayer aquifer systems.

The semi-arid climatic conditions prevailing in the Sierra de Segura aquifer system, located in the southeastern Iberian Peninsula, make this hydrogeological system an excellent natural laboratory for evaluating the suitability of Lc-ex as a tracer of aquifer functioning in dryland environments. The Sierra de Segura hydrogeological system comprises two superposed carbonate aquifers developed within Cretaceous and Jurassic formations, separated by the semi-permeable Utrillas Formation (Dabrio, 1973; López Garrido, 1973; Luque, 2002; Moral, 2005; Morales González et al., 2026). Under this conceptual model, recharge first enters the Upper Cretaceous aquifer and subsequently contributes to the underlying Jurassic aquifer, promoting the progressive attenuation of atmospheric isotopic variability. In this study, we hypothesize that the seasonal variability of Lc-ex decreases progressively from precipitation to the Upper Cretaceous aquifer and subsequently to the Jurassic aquifer, reflecting increasing levels of hydrological integration within the aquifer system. To test this hypothesis, precipitation and groundwater isotope data ($\delta^{18}O$, $\delta^{2}H$, d-ex, and Lc-ex) were jointly analysed to evaluate the potential of Lc-ex as an indicator of recharge processes and isotopic signal attenuation in multilayer Mediterranean semi-arid aquifer system.

A key strength of this study is the spatially and temporally resolved isotope dataset generated across the Sierra de Segura aquifer system (Morales González et al., 2026b). This paired precipitation–groundwater monitoring strategy provides a continuous observational framework to characterize the isotopic variability of atmospheric inputs and to assess how this signal is progressively modified during recharge and groundwater circulation. The combination of event-based precipitation sampling with repeated groundwater observations over multiple years is particularly valuable for distinguishing short-term hydroclimatic variability from longer-term effects of mixing, storage, and hydrological integration. Beyond its application in the present

https://doi.org/10.5194/essd-2026-779
Preprint. Discussion started: 23 November 2026
© Author(s) 2026. CC BY 4.0 License.



Open Access Earth System Science Data Discussions

study, the dataset provides a reference for isotope-based investigations of recharge dynamics and aquifer connectivity in Mediterranean mountain and karst systems.

2. Study Area

The Sierra de Segura is located in the northeastern sector of Jaén Province (southern Spain), within the Betic Cordillera and the Sierras de Cazorla, Segura y Las Villas Natural Park, the largest protected area in Spain (Fig. 1). The study area belongs to the Internal Prebetic Domain of the External Zones of the Betic System, where extensive Jurassic and Cretaceous carbonate formations constitute the main groundwater reservoirs in southeastern Spain.

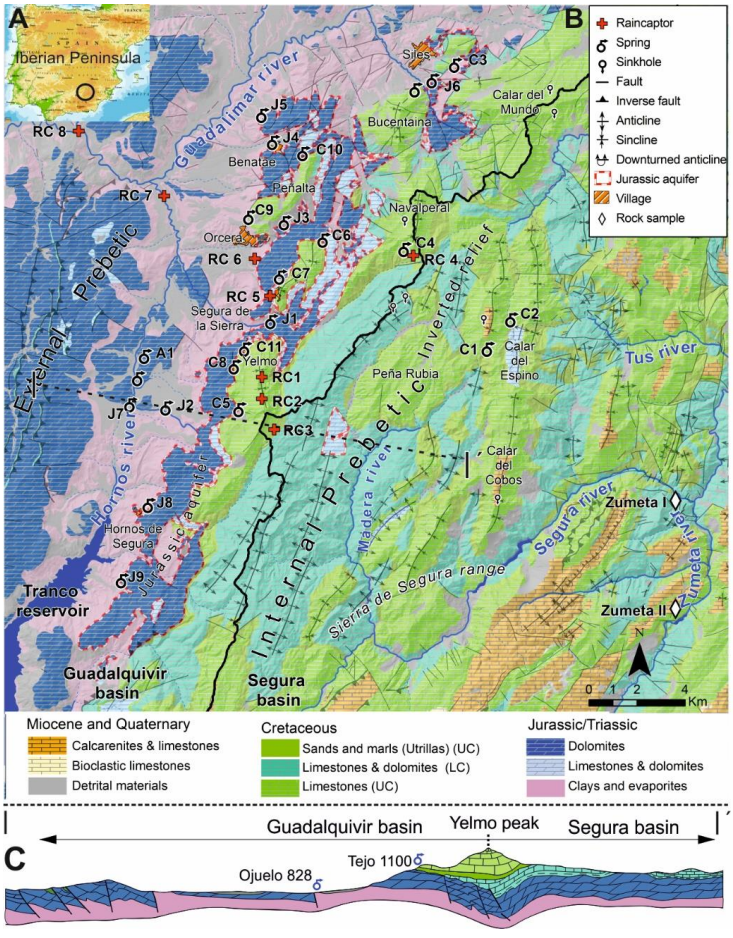

Figure 1. (A) Geographic location of the study area. (B) Geological map of the study area. (C) Geological cross-section I–I' (modified from López Garrido, 1973).

The area is characterized by a Mediterranean mountain climate with marked seasonality in terms of precipitation, temperature and evapotranspiration (Fig.2). Most rainfall occurs between autumn and spring, whereas summers are dry and associated with high evaporative demand. The mean precipitation is approximately 790 mm/yr, and potential evapotranspiration exceeds 1400 mm/yr, concentrating effective recharge during the cool and humid seasons (Morales González, 2018).

https://doi.org/10.5194/essd-2026-779
Preprint. Discussion started: 23 November 2026
© Author(s) 2026. CC BY 4.0 License.

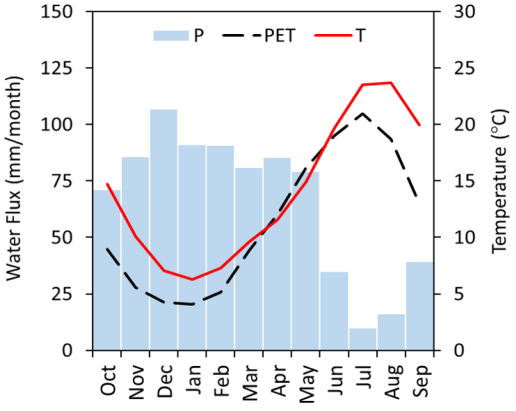

Figure 2. Seasonal patterns of precipitation (P), potential evapotranspiration (PET) and temperatre (T) across the study area. Data were compiled from 70 meteorological stations (Morales González, 2018) covering the period 1970-2023.

The geological succession is dominated by Jurassic, lower and Upper Cretaceous carbonate rocks separated by the Utrillas formation (U-Fm), a siliciclastic unit composed mainly of sand and sandstone. Although traditionally regarded as a hydraulic barrier, the U-Fm behaves as a semi-permeable unit that allows partial hydraulic transfer between adjacent aquifers (Fig 3). The hydrogeological system comprises two vertically superposed carbonate aquifers with contrasting hydraulic behaviors: a highly karstified Upper Cretaceous aquifer characterized by rapid recharge responses and limited storage, and a more extensive Jurassic aquifer with a greater storage capacity and longer groundwater flow paths (Morales González et al., 2026).

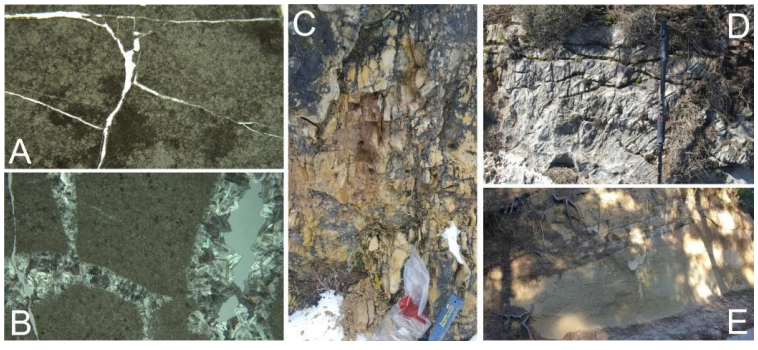

Figure 3. Structural and hydrogeological features of the Sierra de Segura aquifer system. (A) Fracture network developed Jurassic rocks. (B) Calcite-filled fracture illustrating secondary mineralization associated with Cretaceous groundwater circulation. (C) Intensely fractured in Jurassic carbonate outcrop evidencing tectonic control on permeability. (D) Fractured and stratified carbonate sequence representative of the Cretaceous karstified aquifer units. (E) Sandy deposits of the U-Fm, interpreted as a semi-permeable unit that facilitates hydraulic transfer between the Upper Cretaceous and Jurassic aquifers.

Under this conceptual framework, recharge first enters the Upper Cretaceous aquifer and is subsequently transferred, at least partially, to the underlying Jurassic aquifer through the U-Fm This sequential recharge pathway promotes the progressive attenuation of the atmospheric isotopic signal through mixing and groundwater storage, making the Sierra de Segura an ideal natural laboratory for investigating groundwater mixing and storage using Lc-ex.

https://doi.org/10.5194/essd-2026-779
Preprint. Discussion started: 23 November 2026
© Author(s) 2026. CC BY 4.0 License.



3. Materials and Methods

3.1 Spatiotemporal coverage and sampling network

A monitoring programme was conducted in the Sierra de Segura multilayer karst aquifer system between May 2017 and October 2023 to characterize the stable isotope composition of precipitation and groundwater. The resulting dataset comprises 884 water samples, including 403 precipitation samples collected using eight precipitation collectors distributed along an altitudinal transect between 550 and 1800 m a.s.l. (Fig. 1), and 481 groundwater samples collected from 20 springs associated with the Upper Cretaceous and Jurassic carbonate aquifers. Eleven springs drain the Upper Cretaceous aquifer and nine drain the Jurassic aquifer.

The precipitation and groundwater components of the monitoring programme were designed to characterize the temporal variability of the isotopic composition of atmospheric inputs and its representation in groundwater. The precipitation record consists of individual rainfall events, whereas groundwater sampling was conducted repeatedly at the selected springs during the monitoring period.

3.2 Precipitation sampling and sample preparation

Precipitation was collected as the total volume accumulated during each individual rainfall event. At the end of each event, the collected water was sampled and the precipitation collector was reinstalled for the subsequent event. A quantity of liquid paraffin was added to each collector to minimize evaporation and associated isotopic fractionation during the period between rainfall collection and sampling.

After collection, precipitation samples were processed at the Hydrogeology Laboratory of the University of Jaén, where the water was separated from the paraffin layer and the samples were filtered. The filtered water was transferred to 10 mL polypropylene vials and stored under refrigerated conditions until shipment to the Stable Isotope Laboratory of the University of Almería for isotopic analysis.

3.3 Groundwater sampling and sample preservation

Groundwater sampling comprised 21 sampling campaigns conducted between May 2020 and October 2023 at 20 springs associated with the main carbonate aquifer systems of the Sierra de Segura. Eleven springs were associated with the Upper Cretaceous aquifer and nine with the Jurassic aquifer. A total of 481 groundwater samples were collected during the monitoring period.

Groundwater samples were characterized using stable isotope parameters. After collection, samples were filtered in the laboratory and transferred to 5 mL polypropylene vials filled to the brim to minimize air exchange. The samples were refrigerated until analytical processing.

3.4 Stable isotope analyses

Water samples were collected in polypropylene bottles and stored in a refrigerator until analysis. The rainfall collectors were equipped with a layer of liquid paraffin to minimize post-depositional evaporation. Oxygen and hydrogen isotope ratios ($\delta^{18}O$ and $\delta^{2}H$) were determined using a Picarro L2140-i CRDS analyser at the Stable Isotope Laboratory of the University of Almería. The results were normalized to the VSMOW scale using internal laboratory standards analyzed before and after each analytical sequence, as described by Morales González et al. (2024). The long-term precision (1σ) of oxygen and hydrogen isotope analyses were evaluated by measuring an internal standard for every 5–6 samples and was ± 0.1 ‰, and ± 0.6 ‰ for $\delta^{18}O$ and $\delta^{2}H$, respectively (Steig, 2014).

https://doi.org/10.5194/essd-2026-779
Preprint. Discussion started: 23 November 2026
© Author(s) 2026. CC BY 4.0 License.



3.5 Isotopic data analysis

The conceptual model to explain the hydrogeological functioning of the aquifer system is based upon the isotopic composition of precipitation and groundwater, which is analyzed in terms of the variation of both the spatial and seasonal content of $\delta^{18}O$, $\delta^{2}H$, deuterium excess (d-ex), and particularly, local line-conditioned excess (Lc-ex). The isotopic parameters d-ex and Lc-ex are defined as

$$\text{d-ex} = \delta^{2}H - 8\times\delta^{18}O \quad (1)$$

$$\text{Lc-ex} = \delta^{2}H - (a\times\delta^{18}O + b) \quad (2)$$

where a and b represent the slope and intercept of the Local Meteoric Water Line (LMWL) derived from precipitation samples collected in the study area. The d-ex variable quantifies deviations in deuterium abundance from values predicted by a reference isotopic relationship (e.g., V-SMOW), whereas Lc-ex is defined as the deviation in deuterium abundance relative to the Local Meteoric Water Line (LMWL). Both variables are dimensionless and are conventionally reported in per mil (‰).

Environmental tracers (e.g., $\delta^{18}O$ and $\delta^{2}H$) enter the aquifer system through recharge and are transported by groundwater flow. Similarly, d-ex and Lc-ex may also serve as environmental tracers (Custodio, 2019). As these tracers migrate through the aquifer, the temporal variability of the recharge signal is progressively attenuated, resulting in a dampening of its amplitude. This attenuation becomes more pronounced with increasing groundwater transit time (Jódar et al., 2014) and can be observed in the tracer signatures of groundwater emerging at discharge zones (e.g., springs).

The isotopic composition of meteoric water associated with individual precipitation events was characterized at each of the eight rain collectors installed within the study area. Consequently, a time series of the isotopic composition of precipitation events $\{\delta_P\}$ was obtained for each collector. The mean amplitude of the oscillations in the isotopic composition of precipitation in the study zone ($\overline{A}_{\delta_P}$) was then calculated as follows:

$$\overline{A}_{\delta_P} = \frac{1}{M}\sum_{i=1}^{M}\overline{A}_{\delta_{P_i}} \quad (3)$$

$$\overline{A}_{\delta_{P_i}} = \frac{1}{N_i}\sum_{j=1}^{N_i}\varepsilon_{P_{ij}} \quad (4)$$

$$\varepsilon_{P_{ij}} = \left|\delta_{P_{ij}} - \overline{\delta}_{P_i}\right| \quad (5)$$

where $\overline{A}_{\delta_{P_i}}$ is the mean amplitude of the oscillations in the isotopic composition time series associated with the *i*th precipitation collector, M is the number of collectors, N_i is the number of precipitation events sampled at *i*th collector, the $\varepsilon_{P_{ij}}$ denotes the absolute residual between the isotopic composition of the *j*th precipitation event at the ith collector ($\delta_{P_{ij}}$) and the mean isotopic composition of the ith collector ($\overline{\delta}_{P_i}$).

Analogously, the mean amplitude of the temporal variation in the isotopic composition of groundwater ($\overline{A}_{\delta_{GW}}$) within a given aquifer (e.g., the Cretaceous aquifer) is defined as:

https://doi.org/10.5194/essd-2026-779
Preprint. Discussion started: 23 November 2026
© Author(s) 2026. CC BY 4.0 License.



$$\overline{A}_{\delta_{GW}} = \frac{1}{R}\sum_{i=1}^{R}\overline{A}_{\delta_{GW_i}} \quad (6)$$

$$\overline{A}_{\delta_{GW_i}} = \frac{1}{S_i}\sum_{j=1}^{S_i}\varepsilon_{GW_{ij}} \quad (7)$$

$$\varepsilon_{GW_{ij}} = \left|\delta_{GW_{ij}} - \overline{\delta}_{GW_i}\right| \quad (8)$$

where $\overline{A}_{\delta_{GW_i}}$ represents the mean amplitude of the isotopic composition fluctuations observed in the time series of the *i*th sampled spring; R is the total number of springs draining the aquifer, S_i is the number of groundwater samples collected from the *i*th spring; and $\varepsilon_{GW_{ij}}$ is the absolute residual between the isotopic composition of the *j*th groundwater sample from the *i*th spring ($\delta_{GW_{ij}}$) and the mean groundwater isotopic composition of that spring ($\overline{\delta}_{GW_i}$).

3.6. Isotopic indices of temporal integration

Although well-established methods are available for characterizing aquifer renewal time using environmental tracers and lumped-parameter approaches (e.g., Maloszewski and Zuber, 1982; McGuire and McDonnell, 2006; Kirchner, 2016), their application generally requires well-defined tracer input functions, sufficiently resolved time series, and/or site-specific modelling.

To compare the impact of the aquifer system on the isotopic signal of recharge three dimensionless hydroisotopic indices were developed based on Lc-ex variability:

(1) Isotopic Environmental Integration Index (IEI), that describes the relative transformation of the mean Lc-ex signal from precipitation to groundwater

$$IEI = \overline{Lc\text{-}ex}_{GW}/\overline{Lc\text{-}ex}_{P} \quad (9)$$

where $\overline{Lc\text{-}ex}_{GW}$ and $\overline{Lc\text{-}ex}_{P}$ are the mean Lc-ex values of groundwater and precipitation, respectively. The index IEI is used here as a relative descriptor of the modification of the precipitation-derived isotopic signal within the groundwater system.

(2) Isotopic Attenuation Factor (IAF), that expresses the fraction of the precipitation Lc-ex variability preserved in groundwater:

$$IAF = \overline{A}_{Lc_{GW}}/\overline{A}_{Lc_{P}} \quad (10)$$

where $\overline{A}_{Lc_{GW}}$ and $\overline{A}_{Lc_{P}}$ represent the mean amplitude of the Lc-ex variability for groundwater and precipitation, respectively. Lower IAF values indicate stronger attenuation of the precipitation-derived isotopic signal, whereas values approaching unity indicate greater preservation of the original variability.

(3) Temporal Integration Index (TII), that expresses the relative degree of aquifer integration achieved by the isotopic signal as a combined result of groundwater mixing, storage, and isotopic signal integration within the aquifer system.

https://doi.org/10.5194/essd-2026-779
Preprint. Discussion started: 23 November 2026
© Author(s) 2026. CC BY 4.0 License.



Open Access Earth System Science Data Discussions

$$TII = |\overline{Lc\text{-}ex}_{GW}|/\overline{A}_{Lc_{GW}} \quad (11)$$

Higher TII values indicate a groundwater isotopic signal with low temporal variability relative to its mean deviation from the LMWL, reflecting a greater degree of temporal integration. TII increases as seasonal isotopic fluctuations become progressively attenuated relative to the mean groundwater isotopic composition, highlighting the dominant influence of long-term storage and mixing processes over short-term recharge variations. Within the comparative framework proposed here, high TII values denote stronger integration of the isotopic signal, whereas low values indicate greater preservation of short-term variability. Consequently, TII should be interpreted as a relative descriptor of isotopic signal integration rather than a proxy for groundwater age or mean transit time.

These indices are not intended to estimate groundwater age or mean transit time; rather, they provide comparative measures of isotopic signal transformation, attenuation, and temporal integration by within a given aquifer. In this sense, the were interpreted comparatively within the Sierra de Segura aquifer system.

4. Results

The isotopic composition of precipitation (Fig. 4A) exhibits pronounced seasonal variability, primarily reflecting atmospheric controls on rainfall formation and modification. This variability is particularly evident during summer, when precipitation displays the most enriched $\delta^{18}O$ and $\delta^{2}H$ values (Figs. 4B and 5), together with the lowest d-excess and local deuterium excess (Lc-ex) values (Figs. 5C and 5D). Because Lc-ex quantifies deviations from the Local Meteoric Water Line (LMWL), these negative values indicate a substantial influence of sub-cloud evaporation on summer precipitation, consistent with the reduced slope of the summer LMWL (Fig. 4C).

The seasonal evolution of Lc-ex therefore identifies summer rainfall as the most isotopically modified component of the precipitation regime. In contrast, autumn and winter precipitation is characterized by Lc-ex values close to zero or slightly positive, suggesting rainfall that more closely reflects local isotopic equilibrium conditions and is consequently less affected by evaporative fractionation.

https://doi.org/10.5194/essd-2026-779
Preprint. Discussion started: 23 November 2026
© Author(s) 2026. CC BY 4.0 License.

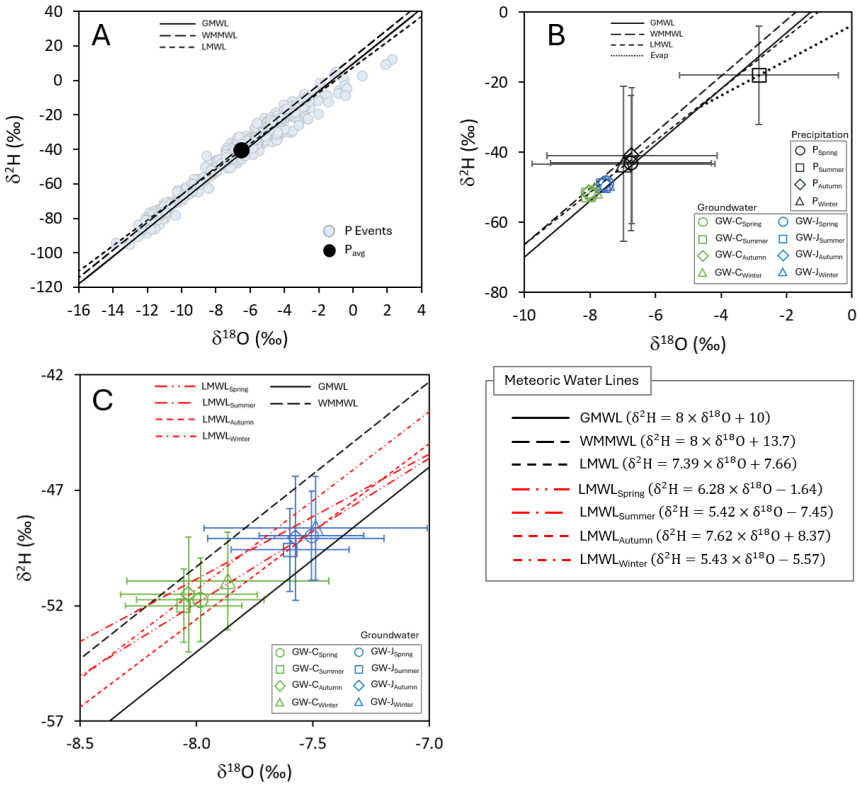

Figure 4. (A) $\delta^{18}O$-δ^2H diagram of the sampled precipitation events. The black symbol represents the mean isotopic composition of the entire precipitation dataset. GMWL, WMMWL, and LMWL denote the Global Meteoric Water Line (Craig, 1961), the Western Mediterranean Meteoric Water Line (Celle-Jeanton et al., 2001), and the Local Meteoric Water Line, respectively. (B) $\delta^{18}O$-δ^2H diagram showing the mean seasonal isotopic composition of precipitation (black symbols) and groundwater from the Cretaceous (GW-C; green symbols) and Jurassic (GW-J; blue symbols) aquifers. Error bars represent ±1 standard deviation. The dotted line indicates a theoretical evaporation line with a slope of 5 passing through the mean isotopic composition of summer precipitation. (C) Enlarged view of the groundwater isotopic composition (green and blue symbols for the Cretaceous and Jurassic aquifers, respectively). In addition to the GMWL and WMMWL, the seasonal Local Meteoric Water Lines (LMWLs) for spring, summer, autumn, and winter are shown in red

In contrast to precipitation, the marked seasonal variability in Lc-ex is not observed in groundwater. Both the Cretaceous and Jurassic aquifers exhibit remarkably stable Lc-ex values throughout the year, varying within a narrow range around zero (Fig. 5D). This stability contrasts sharply with the large seasonal fluctuations recorded in precipitation and indicates that the evaporative imprint characteristic of summer rainfall is largely absent from groundwater.

https://doi.org/10.5194/essd-2026-779
Preprint. Discussion started: 23 November 2026
© Author(s) 2026. CC BY 4.0 License.

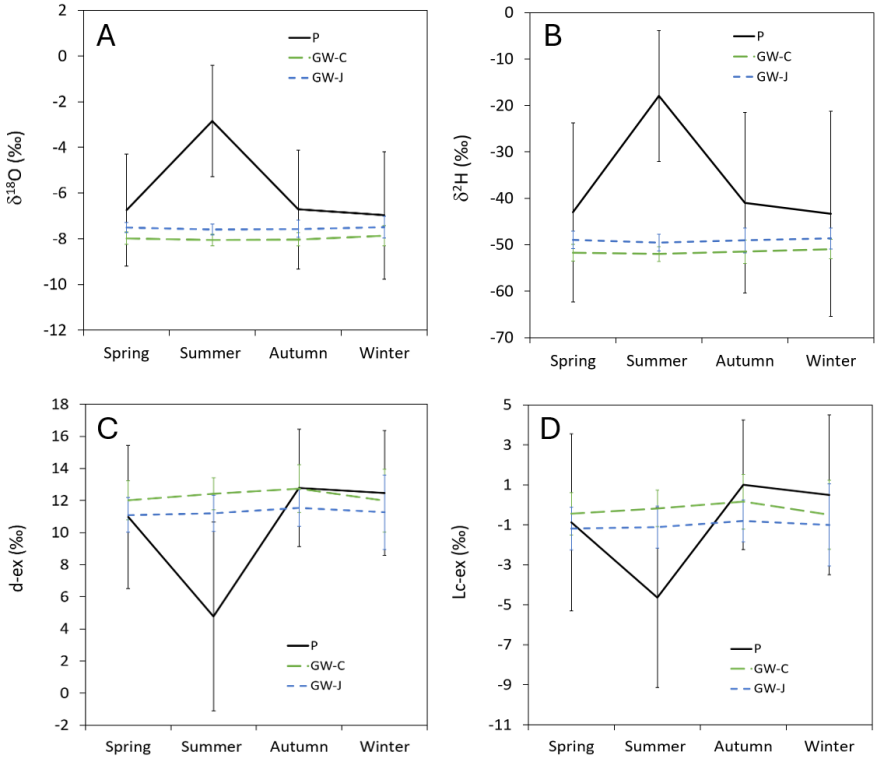

Figure 5. Seasonal variation of $\delta^{18}O$ (A), $\delta^{2}H$ (B), d-ex (C), and Lc-ex (D) *in precipitation and groundwater from the Cretaceous and the Jurassic aquifers. The error bars indicate one standard deviation.*

The absence of negative Lc-ex values in groundwater is particularly informative. If summer precipitation contributed substantially to effective recharge, the isotopically enriched and Lc-ex-depleted signature observed in rainfall would be expected to be reflected, at least to some extent, in groundwater. Instead, groundwater Lc-ex values remain relatively constant throughout the hydrological year, and they consistently fall within the range associated with precipitation that has undergone limited evaporative modification. This pattern suggests that effective recharge is predominantly derived from precipitation occurring during the wetter seasons, which is characterized by Lc-ex values close to zero. Consequently, the isotopic signature of summer rainfall appears to be underrepresented in groundwater, either because summer precipitation contributes only marginally to deep recharge owing to high evapotranspiration losses, or because its signal is diluted through mixing with larger recharge volumes generated during wetter periods of the year (Fig. 2).

The interpretation derived from Lc-ex is further supported by the distribution of samples in $\delta^{18}O$-$\delta^{2}H$ space. Groundwater samples from both aquifers plot close to the seasonal meteoric water lines defined for spring, autumn, and winter, whereas they show a relative separation from the summer LMWL (Fig. 4C). The lower slope of the summer LMWL reflects the evaporative conditions responsible for the strongly negative Lc-ex values observed in summer precipitation. Collectively, both the seasonal meteoric water lines and the temporal evolution of Lc-ex support the conclusion that summer precipitation does not constitute a major component of the recharge signal expressed in groundwater discharge.

https://doi.org/10.5194/essd-2026-779
Preprint. Discussion started: 23 November 2026
© Author(s) 2026. CC BY 4.0 License.



Furthermore, the isotopic differences between the Cretaceous and Jurassic aquifers are considerably smaller than the seasonal differences observed in precipitation (Fig 5). The statistical distribution of the Lc-ex values (Table 1) confirms the progressive reduction in mean Lc-ex values from precipitation to groundwater. Additionally, both aquifers display nearly identical seasonal patterns (Fig. 5), supporting the existence of strong hydraulic connectivity and a substantial integration of recharge signals within the aquifer system. From this perspective, Lc-ex appears to record the effects of groundwater mixing and storage processes more strongly than the short-term seasonal variability of precipitation inputs.

Table 1. Descriptive statistics of Lc-ex values for precipitation (P), groundwater from the Upper Cretaceous aquifer (GW-C), and groundwater from the Jurassic aquifer (GW-J), including the number of samples (N), mean ($\overline{Lc\text{-}ex}$), maximum ($Lc\text{-}ex_{max}$), minimum ($Lc\text{-}ex_{min}$), and standard deviation ($\sigma_{Lc\text{-}ex}$).

Water Type	N (-)	$\overline{\text{Lc- ex}}$ (‰)	$\text{Lc- ex}_{\text{max}}$ (‰)	$\text{Lc- ex}_{\text{min}}$ (‰)	$\sigma_{\text{Lc-ex}}$ (‰)
P	403	0.16	11.90	-12.79	4.04
GW-C	265	-0.19	9.79	-7.93	1.40
GW-J	216	-1.19	1.02	-10.29	1.49

The variability of Lc-ex in groundwater is similar for both aquifers (Table 1). This variability is expressed, for each aquifer as a whole, in terms of the standard deviation associated with all available Lc-ex values. As this is an aggregated measure, it is not possible to determine whether Lc-ex exhibits any altitudinal dependence within the aquifers. To address this, Figure 6 shows the altitudinal distribution of the annual mean Lc-ex for each spring, grouped according to the aquifer they drain.

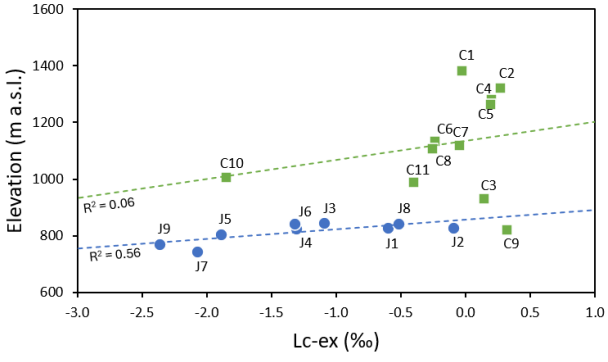

Figure 6. Relationship between mean Lc-ex and spring elevation for the Upper Cretaceous (blue circles) and Jurassic (green squares) aquifers. Dashed lines indicate linear regressions and corresponding R^2 values. The identification codes correspond to those of Fig. 1.

There is a progressive amplitude of the Lc-ex signal from precipitation to the Upper Cretaceous aquifer and subsequently to the Jurassic aquifer (Fig.7A). The Upper Cretaceous and Jurassic aquifers preserve approximately 12% and 9%, respectively, of the seasonal Lc-ex amplitude observed in precipitation, indicating attenuation of approximately from 88% to 91%. This behavior is also observed with other environmental tracers (e.g., $\delta^{18}O$ and $\delta^{2}H$; McGuire and McDonnell, 2006; Harman, 2015; Kirchner, 2016; Jódar et al., 2016; Herms et al., 2019), which show greater attenuation the longer the transit time. Besides, the hydroisotopic indices revealed systematic differences between the groundwater systems (Figs. 7B, 7C and 7D). IEI increased from 0.24 in the Upper Cretaceous aquifer to 1.19 in the Jurassic aquifer. In contrast, IAF

https://doi.org/10.5194/essd-2026-779
Preprint. Discussion started: 23 November 2026
© Author(s) 2026. CC BY 4.0 License.



Open Access Earth System Science Data Discussions

decreased from 0.12 to 0.09, whereas TII increased from 0.59 to 3.91. Together with the amplitude variation (Fig 7A), these patterns indicate a progressive attenuation of the precipitation isotopic signal and increasing temporal integration from precipitation through the Upper Cretaceous to the Jurassic groundwater system.

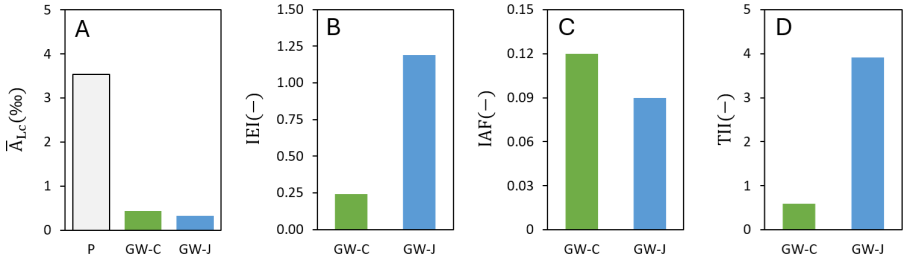

Figure 7. (A) Mean Lc-ex amplitude for precipitation (grey column), and groundwater from the Cretaceous (GW-C; green column) and Jurassic (GW-J; blue column) aquifers. (B) Isotopic environmental integration index for groundwater. (C) Isotopic Attenuation Factor for groundwater. (D) Temporal Integration Index for groundwater.

5. Discussion

The traditional applications of Lc-ex have focused mainly on precipitation, surface waters, and shallow soil water, where it has been used as an indicator of evaporative modification (Landwehr & Coplen, 2006; Sprenger et al., 2017). More recently, Yapiyev et al. (2023) applied Lc-ex to identify recharge and surface water intrusion processes in shallow aquifers in Northern Finland. However, to our knowledge, no previous study has used the progressive attenuation of Lc-ex to evaluate isotopic signal integration within hydraulically connected carbonate aquifers. In this work, Lc-ex is used to profile the aquifer system functioning in terms of the tracer signal transformation from precipitation to groundwater discharge. Whereas precipitation clearly records the influence of sub-cloud evaporation during summer, groundwater maintains relatively stable Lc-ex values close to those expected from the LMWL. This behaviour suggests that recharge comes from precipitation that has experienced limited evaporative modification. Such a pattern is consistent with a karst aquifer system in which recharge is concentrated during the wetter seasons, while mixing and groundwater transit processes efficiently attenuate the isotopic variability of the atmospheric input signal.

The relationship between the mean Lc-ex values and spring discharge elevation (Fig. 6) provides additional insight into the spatial organization of isotopic signals. Springs draining the Upper Cretaceous aquifer generally occupy a distinct isotopic domain characterized by less negative Lc-ex values, whereas Jurassic springs show systematically lower values (Fig. 5), indicative of stronger signal attenuation. However, the relationship between the Lc-ex and altitude differed markedly among the aquifers. The Upper Cretaceous aquifer exhibited virtually no correlation between the two variables ($R^2 = 0.06$), suggesting that local hydrogeological factors dominated the isotopic signatures of individual springs. In contrast, the Jurassic aquifer displayed a moderate positive correlation ($R^2 = 0.56$), indicating a more organized spatial distribution of the isotopic signal, consistent with greater environmental signal integration.

Several Jurassic springs (J1, J8, and particularly J2) displayed Lc-ex values that overlapped with the isotopic domain of the Upper Cretaceous aquifer. Among them, J2 provided the most compelling hydroisotopic evidence of hydraulic transfer between aquifers. Despite discharging from Jurassic formations, its Lc-ex signature is nearly indistinguishable from that of the Upper Cretaceous aquifer, suggesting a substantial contribution of recharge previously integrated within the Upper Cretaceous system before transfer through the U-Fm. Overall, the observed pattern is

https://doi.org/10.5194/essd-2026-779
Preprint. Discussion started: 23 November 2026
© Author(s) 2026. CC BY 4.0 License.



consistent with a stepwise transformation of the atmospheric isotopic signal, whereby the Upper Cretaceous aquifer acts as the initial stage of integration, and the Jurassic aquifer represents a more strongly integrated groundwater reservoir. Therefore, the attenuation of Lc-ex provides a useful indicator of recharge integration, groundwater storage, and hydraulic connectivity in complex, multilayered carbonate aquifer systems.

5.1 IEI, IAF, TII, Limitations of the IEI and the concept of aquifer isotopic memory.

The hydroisotopic indices proposed in this study (i.e., IEI, IAF and TII) provide a comparative framework for describing the progressive transformation of the Lc-ex signal along the precipitation–groundwater continuum. Rather than estimating groundwater age or mean transit time, these indices characterize complementary aspects of isotopic signal evolution, including transformation, attenuation, and temporal integration.

At the aquifer scale, the three indices exhibited a coherent evolution from the Upper Cretaceous to the Jurassic aquifer. IEI increased, IAF decreased, and TII increased markedly along this pathway. Together, these trends indicate progressive transformation and attenuation of the atmospheric isotopic signal and increasing hydrological integration within the groundwater system. Higher IEI values indicate a greater modification of the precipitation-derived Lc-ex signal, decreasing IAF values reflect stronger damping of seasonal Lc-ex variability, and increasing TII values indicate enhanced temporal integration associated with groundwater storage and mixing.

IEI should be interpreted as a relative descriptor of isotopic transformation rather than an absolute metric, because its magnitude depends on the mean Lc-ex value of precipitation. Consequently, the proposed indices are most useful for evaluating relative differences in isotopic signal preservation within the same hydroclimatic framework.

An additional limitation of the IEI index is that the mean precipitation Lc-ex values were relatively close to zero. Under these conditions, small variations in groundwater Lc-ex may produce comparatively large changes in IEI values. Therefore, the IEI should not be interpreted as an absolute measure of groundwater transformation but rather as a comparative descriptor of isotopic signal modification within the same hydroclimatic setting. Its value lies primarily in identifying relative differences in isotopic integration among springs and aquifer units exposed to similar climatic forces.

The progressive attenuation of Lc-ex variability observed from precipitation to groundwater can also be interpreted in terms of aquifer isotopic memory, defined here as the capacity of a groundwater system to preserve information about the isotopic characteristics of recharge despite the effects of storage and mixing. Within this framework, precipitation serves as the initial climatic signal, whereas groundwater progressively integrates and transforms this signal during the subsurface circulation. Therefore, isotopic memory should be regarded as an emergent property of groundwater mixing and storage, rather than a direct measure of groundwater age or mean transit time.

The interpretation of the proposed indices is consistent with previous studies showing that that tracer attenuation increases with groundwater storage, mixing, and flow path integration (McGuire and McDonnell, 2006; Harman, 2015; Kirchner, 2016). The systematic evolution of the IEI, IAF, and TII in the Sierra de Segura indicates a transition from a relatively responsive recharge system in the Upper Cretaceous aquifer to a more integrated groundwater reservoir in the Jurassic Aquifer.

Although the proposed indices do not provide direct estimates of groundwater age or mean transit time, they offer a simple and reproducible approach for comparing signal attenuation between springs and aquifers. Beyond the Sierra de Segura, this framework may help identify recharge

https://doi.org/10.5194/essd-2026-779
Preprint. Discussion started: 23 November 2026
© Author(s) 2026. CC BY 4.0 License.



pathways, evaluate groundwater storage behaviour, and assess hydraulic connectivity in other multilayer aquifer systems

5.2. Implications for groundwater management and the resilience of stratified aquifer systems under climate change

The contrasting hydroisotopic behaviors of the Upper Cretaceous and Jurassic aquifers have direct implications for groundwater management under increasing climatic variability. Aquifer systems characterized by lower signal damping respond more rapidly to recharge fluctuations, but they are also more sensitive to changes in precipitation, seasonality, evaporative demand, and prolonged droughts. Conversely, highly integrated aquifer systems buffer short-term climatic variability through larger effective storage volumes and enhanced groundwater mixing, although this increased inertia may result in slower responses to long-term environmental changes (McGuire and McDonnell, 2006; Taylor et al. 2013;Kirchner, 2016).

The progressive attenuation of the Lc-ex signal observed from precipitation to the Jurassic aquifer reflects an increasing degree of groundwater integration that extends beyond isotope evolution alone. Greater groundwater storage and longer effective flow paths enhance the capacity of the aquifer system to buffer climatic variability by reducing seasonal fluctuations in recharge and sustaining groundwater discharge during dry periods. Similar hydrological buffering processes have been described in mountain karst aquifers, where groundwater storage represents the dominant control on discharge persistence despite rapid recharge events (Jódar et al., 2020).

The hydrogeological functioning inferred from the proposed "SHOWER EFFECT" (Morales González et al., 2026) therefore has implications that extend beyond groundwater flow dynamics. Hydraulic transfer between superposed aquifers increases the effective storage capacity of the regional groundwater system, enhancing its resilience to declining recharge and increasing drought frequency. Such behaviour is particularly relevant in Mediterranean regions, where climate projections indicate reduced recharge and increased hydrological variability (Giorgi, 2006; Kjellström et al., 2013). Consequently, groundwater storage should be regarded not only as a strategic water resource but also as a key component supporting groundwater-dependent ecosystems and ecosystem resilience under climate change (Goldscheider et al., 2020; Hartmann et al., 2021).

From this perspective, the degree of progressive signal modification inferred from the Lc-ex can be regarded as an indicator of aquifer resilience. In the Sierra de Segura, the Jurassic aquifer exhibited the highest degree of isotopic integration and therefore appeared to function as a strategic groundwater reservoir capable of mitigating the effects of interannual climatic variability on water supply. In contrast, the Upper Cretaceous aquifer retains a stronger imprint of recent recharge and is expected to respond more rapidly to future changes in recharge conditions. Similar links between groundwater storage capacity, climatic buffering, and resilience to hydroclimatic stress have been highlighted in recent studies that addressed groundwater responses to climate change (Taylor et al., 2013; Cuthbert et al., 2019; Jódar et al., 2025).

The evidence for hierarchical recharge between the Upper Cretaceous and Jurassic aquifers further highlights the need to manage them as a single, interconnected hydrogeological system, rather than as independent groundwater bodies. Variations in recharge affecting the Upper Cretaceous aquifer may ultimately influence the quantity and quality of groundwater discharged from the Jurassic aquifer through hydraulic transfer across the U-Fm. This perspective is consistent with the concept that hydraulically connected groundwater systems should be considered and managed as integrated water resources (Winter et al., 1998; Sophocleous, 2002).

The conceptual framework proposed in this study may therefore be applicable to other multilayer carbonate aquifer systems where hydraulic connectivity promotes progressive groundwater mixing and storage. In this context, Lc-ex provides information not only on post-condensation processes but also on the degree of hydrological integration achieved within the aquifer system.

https://doi.org/10.5194/essd-2026-779
Preprint. Discussion started: 23 November 2026
© Author(s) 2026. CC BY 4.0 License.



The proposed hydroisotopic indices (IEI, IAF and TII) offer complementary tools for assessing groundwater storage behaviour, recharge dynamics and hydraulic resilience under changing climatic conditions.

6. Data availability: The dataset presented in this study is openly available through Zenodo under DOI 10.5281/zenodo.22903603 (Morales-González et al., 2026b). The repository provides the precipitation and groundwater stable isotope observations together with the associated sampling information and derived variables described in this study.

7. Conclusions

The isotopic dataset collected in the Sierra de Segura shows that Lc-ex is particularly effective for identifying hydroclimatic variability and following the evolution of the precipitation signal during recharge and groundwater circulation. Compared with $\delta^{18}O$, $\delta^{2}H$, and d-excess, Lc-ex retains information related to post-condensation processes while simultaneously reflecting the effects of mixing and storage within the aquifer system.

Lc-ex appears to provide information not only on evaporative processes but also to the extent to which recharge has been mixed and homogenized during groundwater circulation. The results revealed a progressive increase in hydrological integration from precipitation to groundwater. The Upper Cretaceous aquifer preserves part of the variability inherited from recharge whose propagation is favoured by the karstification degree of the Cretaceous formation. The Jurassic aquifer displays a more homogeneous isotopic response, consistent with longer storage and greater mixing. The Lc-ex results reinforce the conceptual model of connectivity between the two aquifers through the U-Fm.

The hydroisotopic indices proposed in this study (IEI, IAF, and TII) provide a simple method for comparing the degree of isotopic transformation among springs and aquifers. These indices quantify the extent to which the original atmospheric signal has been modified by subsurface processes such as storage, mixing, and temporal integration, allowing meaningful comparisons between hydrogeological units with different flow characteristics.

Author contributions: Conceptualization: A.L.M.G., A.G.R., and J.J.; Methodology: A.L.M.G., A.G.R., and J.J.; Software, A.L.M.G.; Validation: J.J., R.J.E., F.G. and F.M.M.; Formal Analysis: J.J.; Investigation: A.L.M.G.; Resources: A.L.M.G. and F.G.; Data Curation: A.L.M.G., J.J. and A.G.R.; Writing—Original Draft Preparation: A.L.M.G., J.J. and A.G.R.; Writing—Review and Editing: A.L.M.G. and J.J.; Visualization: A.L.M.G. Supervision: R.J.E., F.M.M., F.G., J.J. and A.G.R.; Project Administration: A.L.M.G.;

Competing interests: The authors declare no conflicts of interest. The funders had no role in the design of the study; in the collection, analyses, or interpretation of data; in the writing of the manuscript; or in the decision to publish the results.

Disclaimer: Copernicus Publications adds a standard disclaimer: “Copernicus Publications remains neutral with regard to jurisdictional claims made in the text, published maps, institutional affiliations, or any other geographical representation in this paper. While Copernicus Publications makes every effort to include appropriate place names, the final responsibility lies with the authors. Views expressed in the text are those of the authors and do not necessarily reflect the views of the publisher.”

Acknowledgements: The authors thank the University of Jaén, the University of Almería, and the Geological Service of Spain (IGME-CSIC) for their institutional support.

https://doi.org/10.5194/essd-2026-779
Preprint. Discussion started: 23 November 2026
© Author(s) 2026. CC BY 4.0 License.



Financial support: This research was supported by the AQUAKARST project (PLSQ-2023–00284), H2RISE (PID2024–161600OB-I00) and co-financed by FEDER, EU, and the research project PID2024-158529NB-I00.

References:

Araguás-Araguás, L., Froehlich, K., & Rozanski, K. (2000). Deuterium and oxygen-18 isotope composition of precipitation and atmospheric moisture. Hydrological Processes, 14(8), 1341–1355. https://doi.org/10.1002/1099-1085(20000615)14:8<1341::AID-HYP983>3.0.CO;2-Z

Bouchaou, L., El Alfy, M., Shanafield, M., Siffeddine, A., & Sharp, J. (2024). Groundwater in Arid and Semi-Arid Areas. Geosciences, 14, 332. https://doi.org/10.3390/geosciences14120332

Clark, I. D., & Fritz, P. (1997). Environmental Isotopes in Hydrogeology. Lewis Publishers, Boca Raton, FL. https://library.usi.edu/record/467028

Cardona-Hernández, J., Esquivel-Hernández, G., Rebelo Monteiro, L., Sánchez-Murillo, R., Cotrim, M. E. B., Sánchez-Gutiérrez, R., Birkel, C., Peña-Paz, T., & Benegas-Negri, L. A. (2026). Isotope-informed water sources and recharge mechanisms in a tropical karst environment of the Talgua River Basin, Honduras. Journal of South American Earth Sciences, 170, 105891. https://doi.org/10.1016/j.jsames.2025.105891

Celle-Jeanton, H., Travi, Y., & Blavoux, B. (2001). Isotopic typology of the precipitation in the Western Mediterranean region at three different time scales. Geophysical research letters, 28(7), 1215-1218. https://doi.org/10.1029/2000GL012407

Craig, H. (1961). Isotopic variations in meteoric waters. Science, 133(3465), 1702-1703. https://www.science.org/doi/10.1126/science.133.3465.1702

Custodio, E. (2019). Recarga natural a los acuíferos, metodología y soporte de la isotopía del agua. Aplicación a la planificación hidrológica y conocimiento de las aguas subterráneas en España. Informe RAEMIA. Universitat Politècnica de Catalunya, Barcelona. 1200+ pp. ISBN 978-84-9880-814-8. DOI: 10.5821/ebook-9788498808148

Cuthbert, M.O., Taylor, R.G., Favreau, G., Todd, M.C., Shamsudduha, M., Villholth, K.G., MacDonald, A.M., Scanlon, B.R., Kotchoni, D.O.V., Vouillamoz, J.-M., Lawson, F.M.A., Adjomayi, P.A., Kashaigili, J., Seddon, D., Sorensen, J.P.R., Ebrahim, G.Y., Owor, M., Nyenje, P.M., Nazoumou, Y., Goni, I., Ousmane, B.I., Sibanda, T., Ascott, M.J., Macdonald, D.M.J., Agyekum, W., Koussoubé, Y., Wanke, H., Kim, H., Wada, Y., Lo, M.-H., Oki, T., & Kukuric, N. (2019). Observed controls on resilience of groundwater to climate variability in sub-Saharan Africa. Nature, 572(7768), 230–234. https://doi.org/10.1038/s41586-019-1441-7

Dabrio, C. J.: Geología del Sector del Alto Segura (Zona Prebética), Doctoral dissertation, Universidad de Granada, Granada, Spain, 1973. https://ccbe.feec.cat/index.php?id=7517&lvl=notice_display

Dansgaard, W. (1964). Stable isotopes in precipitation. Tellus, 16(4), 436–468. https://doi.org/10.1111/j.2153-3490.1964.tb00181.x

Froehlich, K., Gibson, J. J., & Aggarwal, P. (2002). Deuterium excess in precipitation and its climatological significance. Proceedings of the International Atomic Energy Agency (IAEA). https://www-pub.iaea.org/MTCD/Publications/PDF/CSP_26_web.pdf

Gat, J. R. (1996). Oxygen and hydrogen isotopes in the hydrologic cycle. Annual Review of Earth and Planetary Sciences, 24, 225–262. Ghosh, A., Pant, D., Kajla, M., et al. (2025). Isotope characterisation of groundwater resources in uranium impacted Fazilka, Punjab. Journal of Radioanalytical and Nuclear Chemistry, 334, 4243–4250. https://doi.org/10.1146/annurev.earth.24.1.225

Ghosh, A., Pant, D., Kajla, M., Mohokar, H., Jaryal, A., & Keesari, T. (2025). Isotope characterisation of groundwater resources in uranium impacted Fazilka, Punjab. Journal of Radioanalytical and Nuclear Chemistry, 334(6), 4243–4250. https://doi.org/10.1007/s10967-024-09739-5

Giorgi, F. (2006). Climate change hot-spots. Geophys. Res. Lett. 33, 1–4. https://doi.org/10.1029/2006GL025734

Goldscheider, N.; Chen, Z.; Auler, A. S.; Bakalowicz, M.; Broda, S.; Drew, D.; Hartmann, J.; Jiang, G.; Moosdorf, N.; Stevanovic, Z.; et al.: Global distribution of carbonate rocks and karst

https://doi.org/10.5194/essd-2026-779
Preprint. Discussion started: 23 November 2026
© Author(s) 2026. CC BY 4.0 License.



569 water resources, Hydrogeol. J., 28, 1661–1677, 2020. https://doi.org/10.1007/s10040-020-
570 02139-5
571 Hartmann, A.; Jasechko, S.; Gleeson, T.; Wada, Y.; Andreo, B.; Barbera, J. A.; Brielmann, H.;
572 Bouchaou, L.; Charlier, J. B.; Darling, W. G.; et al.: Risk of groundwater contamination widely
573 underestimated because of fast flow into aquifers, Proc. Natl. Acad. Sci. USA, 118,
574 e2024492118, 2021. https://doi.org/10.1073/pnas.2024492118
575 Harman, C. J.: Time-variable transit time distributions and transport: theory and application to
576 storage-dependent transport of chloride in a watershed, Water Resour. Res., 51, 1–30,
577 https://doi.org/10.1002/2014WR015707, 2015.
578 Herms, I.; Jódar, J.; Soler, A.; Lambán, L. J.; Custodio, E.; Núñez, J. A.; Arnó, G.; Parcerisa, D.;
579 Jorge-Sánchez, J.: Contribution of isotopic research techniques to characterize high-mountain-
580 Mediterranean karst aquifers: the Port del Comte (Eastern Pyrenees) aquifer, Sci. Total
581 Environ., 656, 209–230, https://doi.org/10.1016/j.scitotenv.2018.11.188, 2019.
582 Jódar, J., Lambán, L.J., Medina, A., Custodio, E., (2014): Exact analytical solution of the
583 convolution integral for classical hydrogeological lumped-parameter models and typical input
584 tracer functions in natural gradient systems. Journal of Hydrology, 519: pp 3275–3289,
585 https://doi.org/10.1016/j.jhydrol.2014.10.027
586 Jódar, J., Custodio, E., Lambán, L. J., Martos-Rosillo, S., Herrera-Lameli, C., & Sapriza-Azuri,
587 G. (2016). Vertical variation in the amplitude of the seasonal isotopic content of rainfall as a
588 tool to jointly estimate the groundwater recharge zone and transit times in the Ordesa and
589 Monte Perdido National Park aquifer system, north-eastern Spain. *Science of the Total*
590 *Environment*, *573*, 505–517. https://doi.org/10.1016/j.scitotenv.2016.08.117
591 Jódar, J., González-Ramón, A., Martos-Rosillo, S., Heredia, J., Herrera, C., Urrutia, J., Caballero,
592 Y., Zabaleta, A., Antigüedad, I., Custodio, E., & Lambán, L.J. (2020). Snowmelt as a
593 determinant factor in the hydrogeological behaviour of high mountain karst aquifers: The
594 Garcés karst system, Central Pyrenees (Spain). Science of the Total Environment, 748,
595 141363. https://doi.org/10.1016/j.scitotenv.2020.141363
596 Jódar, J., Morales-González, A.L., Urrutia, J., Herrera, C., Lambán, L.J., Martos-Rosillo, S., &
597 González-Ramón, A. (2025). Characterisation of mountain-Mediterranean karst aquifers as
598 lighthouses for the assessment of global change impacts in the Mediterranean region: The
599 Sierra Seca aquifer system (SE Spain). Science of the Total Environment, 985, 179719.
600 https://doi.org/10.1016/j.scitotenv.2025.179719
601 Kjellström, E., Thejll, P., Rummukainen, M., Christensen, J. H., Boberg, F., Christensen, O. B.,
602 & Fox Maule, C. (2013). Emerging regional climate change signals for Europe under varying
603 large-scale circulation conditions. *Climate Research*, *56*(2), 103–119.
604 https://doi.org/10.3354/cr01146
605 Kirchner, J. W.: Aggregation in environmental systems – Part 1: seasonal tracer cycles quantify
606 young water fractions, but not mean transit times, in spatially heterogeneous catchments,
607 Hydrol. Earth Syst. Sci., 20, 279–297, https://doi.org/10.5194/hess-20-279-2016, 2016.
608 Kirchner, J. W.: Aggregation in environmental systems – Part 2: catchment mean transit times
609 and young water fractions under hydrologic nonstationarity, Hydrol. Earth Syst. Sci., 20, 299–
610 328, https://doi.org/10.5194/hess-20-299-2016, 2016.
611 Landwehr, J. M., & Coplen, T. B. (2006). Line-conditioned excess: A new method for
612 characterizing stable hydrogen and oxygen isotope ratios in hydrologic systems. In Isotopes
613 in Environmental Studies, IAEA-CN-118/56, 132–135. International Atomic Energy Agency.
614 http://inis.iaea.org/Search/search.aspx?orig_q=RN:37043527
615 López Garrido, A. C.: Mapa Geológico de España, escala 1:50.000, Hoja nº 887 (Orcera);
616 Segunda serie (MAGNA), Instituto Geológico y Minero de España, Madrid, Spain, 1973.
617 https://info.igme.es/catalogo/resource.aspx?catalog=1&ctt=1&dlang=eng&lang=spa&llt=dro
618 pdown&master=datosgobes&portal=1&resource=6984
619 Luque Espinar, J. A.; Cobos Fernández, J. R.: Papel de las formaciones poco permeables en la
620 recarga de los acuíferos de Cazorla-Segura, Quesada-Castril y Segura-Cazorla, in: Presente y
621 Futuro de las Aguas Subterráneas en la Provincia de Jaén, IGME, Madrid, Spain, 407–408,
622 2002.
623 https://web.igme.es/actividadesigme/lineas/HidroyCA/publica/libros3_RHS/Libro108/Lib_1
624 08.htm

https://doi.org/10.5194/essd-2026-779
Preprint. Discussion started: 23 November 2026
© Author(s) 2026. CC BY 4.0 License.



625 Maloszewski, P.; Zuber, A.: Determining the turnover time of groundwater systems with the aid
626 of environmental tracers, J. Hydrol., 57, 207–231, 1982. https://doi.org/10.1016/0022-
627 1694(82)90147-0
628 McGuire, K. J.; McDonnell, J. J.: A review and evaluation of catchment transit time modeling, J.
629 Hydrol., 330, 543–563, https://doi.org/10.1016/j.jhydrol.2006.04.020, 2006.
630 Moral, F.: Contribución al Conocimiento de los Acuíferos Carbonáticos de la Sierra de Segura
631 (Alto Guadalquivir y Alto Segura), Doctoral dissertation, Universidad Pablo de Olavide,
632 Sevilla, Spain, 2005. https://hdl.handle.net/10433/16551
633 Morales-González, A. L., Andreo B., Mudarra M.: Caracterización del medio físico, con énfasis
634 hidrometeorológico, de los acuíferos carbonáticos en la Sierra de Segura (Provincia de Jaén),
635 Trabajo Fin de Máster, Universidad de Málaga, Spain. 2018.
636 Morales-González, A. L., Jódar-Bermúdez, J., Jiménez-Espinosa, R., & González-Ramón, A.
637 (2024). Comparación entre 3 metodologías para la determinación de la altitud del área de
638 recarga de manantiales de la Sierra de Segura (Jaén) basadas en isótopos ambientales.
639 Geogaceta, 76, 51–54. https://doi.org/10.55407/geogaceta104567
640 Morales-González, A.L., Jódar-Bermúdez, J., González-Ramón, A., Moral-Martos, F., Jiménez-
641 Espinosa, R., & Gázquez, F. (2026). Hydrochemical Evidence of Groundwater Transfer
642 Between Karst Aquifers in Southern Spain: Implications for Climate Resilience and
643 Groundwater-Dependent Ecosystems. Water, 18, 2349. https://doi.org/10.3390/w18182349
644 Morales-González A.L., Jódar, J., Jiménez Espinosa, R., González Ramón, A., Moral Martos, F.,
645 Gázquez Sánchez, F. (2026b). Isotopic database for precipitation and groundwater in the Sierra
646 de Segura. Province of Jaén. Spain. DOI: 10.5281/zenodo.22903603.
647 Pfahl, S., & Sodemann, H. (2014). What controls deuterium excess in global precipitation?
648 Climate of the Past, 10, 771–781. https://doi.org/10.5194/cp-10-771-2014
649 Rozanski, K., Araguás-Araguás, L., & Gonfiantini, R. (1993). Isotopic patterns in modern global
650 precipitation. In P. K. Swart, K. C. Lohmann, J. McKenzie, & S. Savin (Eds.), Climate Change
651 in Continental Isotopic Records. Geophysical Monograph Series, 78, 1–36. American
652 Geophysical Union. https://doi.org/10.1029/GM078p0001
653 Siyad, S.A., & Mohamed, Z.H. (2025). A systematic literature review on groundwater recharge
654 dynamics under climate variability, land use change and sea level rise. Discover Sustainability,
655 6, 1331. https://doi.org/10.1007/s43621-025-02232-3
656 Sophocleous, M.: Interactions between groundwater and surface water: the state of the science,
657 Hydrogeol. J., 10, 52–67, https://doi.org/10.1007/s10040-001-0170-8, 2002.
658 Sorensen, J.P.R., Gahi, N.Z., Guug, S., Verhoef, A., Koïta, M., Sandwidi, W.J.P., Agyekum,
659 W.A., Okrah, C., Darling, W.G., Lawson, F.M.A., MacDonald, A.M., Vouillamoz, J.-M., &
660 Macdonald, D.M.J. (2024). Groundwater recharge is diffuse in semi-arid African drylands:
661 Evidence from highly instrumented observatories. Journal of Hydrology, 636, 131227.
662 https://doi.org/10.1016/j.jhydrol.2024.131227
663 Sprenger, M.; Dick, J. J.; Tetzlaff, D.; Buttle, J.; Laudon, H.; Leistert, H.; Mitchell, C. P. J.;
664 Snelgrove, J.; Weiler, M.; Soulsby, C.: Evaporation fractionation in a peatland drainage
665 network affects stream water isotope composition, Water Resour. Res., 53, 684–697,
666 https://doi.org/10.1002/2016WR019258, 2017.
667 Steig, E. J.; Gkinis, V.; Schauer, A. J.; Schoenemann, S. W.; Samek, K.; Hoffnagle, J.; Dennis,
668 K. J.; Tan, S. M.: Calibrated high-precision 17O-excess measurements using cavity ring-down
669 spectroscopy with laser-current-tuned cavity resonance, Atmos. Meas. Tech., 7, 2421–2435,
670 https://doi.org/10.5194/amt-7-2421-2014, 2014
671 Taylor, R. G.; Todd, M. C.; Kongola, L.; Maurice, L.; Nahozya, E.; Sanga, H.; et al.: Evidence of
672 the dependence of groundwater resources on extreme rainfall in East Africa, Nat. Clim.
673 Chang., 3, 374–378, https://doi.org/10.1038/nclimate1731, 2013.
674 Turkeltaub, T., & Bel, G. (2024). Changes in mean evapotranspiration dominate groundwater
675 recharge in semi-arid regions. Hydrology and Earth System Sciences, 28, 4263–4274.
676 https://doi.org/10.5194/hess-28-4263-2024
677 Winter, T. C.; Harvey, J. W.; Franke, O. L.; Alley, W. M.: Ground Water and Surface Water: A
678 Single Resource, U.S. Geological Survey Circular 1139, 79 pp.,
679 https://doi.org/10.3133/cir1139, 1998.

https://doi.org/10.5194/essd-2026-779
Preprint. Discussion started: 23 November 2026
© Author(s) 2026. CC BY 4.0 License.



680 Yanes, J. L., & Moral, F. (2022). Relief and climate influence on isotopic composition of Atlantic-
681 Mediterranean karst spring waters (Andalusia, southern Spain). Hydrological Processes, 36(9),
682 e14669. https://doi.org/10.1002/hyp.14669
683 Yapiyev, V., Rossi, P. M., Ala-Aho, P., & Marttila, H. (2023). Stable Water Isotopes as an
684 Indicator of Surface Water Intrusion in Shallow Aquifer Wells: A Cold Climate Perspective.
685 Water Resources Research, 59, e2022WR033056. https://doi.org/10.1029/2022WR033056
686

687